Author's Accepted Manuscript

www.elsevier.com/locate/talanta

Protein-mimicking nanowire-Inspired Electro-catalytic Biosensor for Probing Acetylcholinesterase Activity and Its Inhibitors

Qingqing Zhang, Yufang Hu, Di Wu, Shaohua Ma, Jiao Wang, Jiajia Rao, Lihua Xu, Huan Xu, Huili Shao, Zhiyong Guo, Sui Wang

PII: S0039-9140(18)30139-5
DOI: https://doi.org/10.1016/j.talanta.2018.02.034
Reference: TAL18353

To appear in: *Talanta*

Received date: 15 December 2017
Revised date: 5 February 2018
Accepted date: 7 February 2018

Cite this article as: Qingqing Zhang, Yufang Hu, Di Wu, Shaohua Ma, Jiao Wang, Jiajia Rao, Lihua Xu, Huan Xu, Huili Shao, Zhiyong Guo and Sui Wang, Protein-mimicking nanowire-Inspired Electro-catalytic Biosensor for Probing Acetylcholinesterase Activity and Its Inhibitors, *Talanta,* https://doi.org/10.1016/j.talanta.2018.02.034

Protein-mimicking nanowire-Inspired Electro-catalytic Biosensor for Probing Acetylcholinesterase Activity and Its Inhibitors

Qingqing Zhang[a], Yufang Hu[a,b*], Di Wu[c], Shaohua Ma[a], Jiao Wang[a], Jiajia Rao[a], Lihua Xu[a], Huan Xu[a], Huili Shao[a], Zhiyong Guo[a], Sui Wang[a]

[a] Faculty of Materials Science and Chemical Engineering, Ningbo University, Ningbo 315211, P. R. China

[b] State Key Laboratory of Chemo/Biosensing and Chemometrics, College of Chemistry and Chemical Engineering, Hunan University, Changsha 410082, P. R. China

[c] The First Hospital of Changsha (Infectious Disease Hospital and Public Health Care Center of Changsha), Changsha 410005, P. R. China

***** Corresponding author. Tel.: +86 574 87600798; Fax: +86 574 87600798. huyufang@nbu.edu.cn

ABSTRACT

A highly sensitive electrochemical biosensor based on the synthetized *L*-Cysteine-Ag(I) coordination polymer (*L*-Cys-Ag(I) CP), which looks like a protein-mimicking nanowire, was constructed to detect acetylcholinesterase (AChE) activity and screen its inhibitors. This sensing strategy involves the reaction of acetylcholine chloride (ACh) with acetylcholinesterase (AChE) to form choline that is in turn catalytically oxidized by choline oxidase (ChOx) to produce hydrogen peroxide (H_2O_2), thus *L*-Cys-Ag(I) CP

possesses the electro-catalytic property to H_2O_2 reduction. Herein, the protein-mimicking nanowire-based platform was capable of investigating successive of H_2O_2 effectively by amperometric *i-t* (current-time) response, and was further applied for the turn-on electrochemical detection of AChE activity. The proposed sensor is highly sensitive (limit of detection is 0.0006 U/L) and is feasible for screening inhibitors of AChE. The model for AChE inhibition was further established and two traditional AChE inhibitors (donepezil and tacrine) were employed to verify the feasibility of the system. The IC_{50} of donepezil and tacrine were estimated to be 1.4 nM and 3.5 nM, respectively. The developed protocol provides a new and promising platform for probing AChE activity and screening its inhibitors with low cost, high sensitivity and selectivity.

Graphical abstract

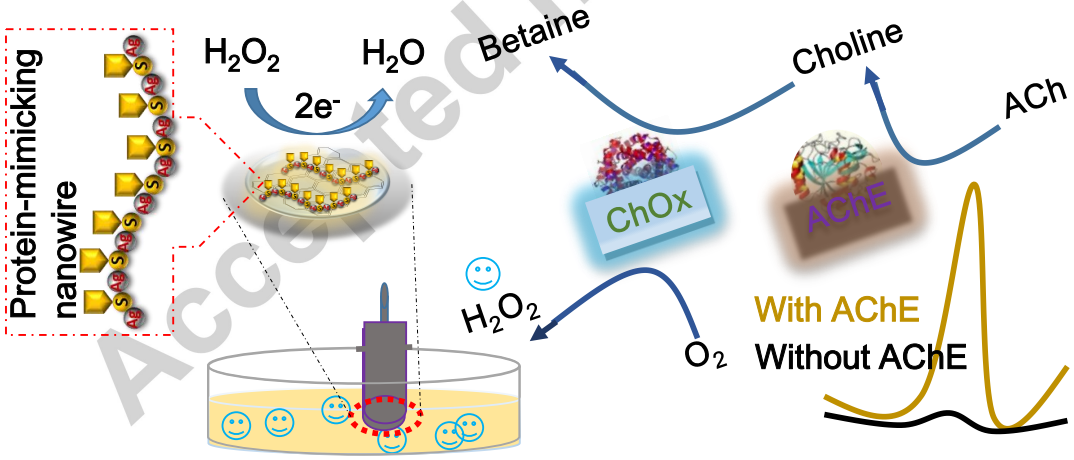

A highly sensitive electrochemical biosensor was constructed to detect acetylcholinesterase (AChE) activity and screen its inhibitors based on *L*-Cys-Ag(I) coordination polymer which looks like a protein-mimicking nanowire with excellent electro-catalytic property to H_2O_2 reduction.

Keywords: *L*-Cys-Ag(I) coordination polymer; Protein-mimicking nanowire; Electro-catalytic property; Acetylcholinesterase; Inhibitor

1. Introduction

Acetylcholinesterase (AChE), as a critical enzyme in the central nervous system, plays a significant role in biological signal transmission, which mainly functions to terminate synaptic transmission at cholinergic synapses through rapid hydrolysis of acetylcholine (ACh) and has pivotal functions in Alzheimer Disease, inflammatory processes and nerve-agent poisoning [1-4]. This enzyme has profoundly widespread importance in healthcare and medicine for a variety of reasons. Inhibition of AChE activity would cause accumulation of ACh in a synaptic cleft, resulting in hindered neurotransmission. Regulating the activity of AChE would have great impact on physiological function. Therefore, the development of efficient approaches for AChE activity measurement with high sensitivity and facile manipulation is of high importance on both theoretical and practical aspects. So far many well-known techniques, including traditional Ellman's method [5], gold nanoparticles-based colorimetric assay [6, 7], synthetic probes-derived fluorescent approaches [8, 9], mass spectrometry [10], enzyme-linked immune-sorbent assay [11], and so on, have been developed to monitor AChE activity and screen its inhibitors. These methods have high selectivity and adequate sensitivity, but these techniques suffer from the disadvantages of high costs, sophisticated instruments and high requirements for testing staff possessing master professional skills and sample pretreatment, resulting

in the fact that they are not suitable for on-site detection in most settings, especially in emergency cases. So, it is still attractive to develop convenient and simple analytical methods for AChE assay.

In the past decade, many novel nano-materials have emerged for probing enzyme-catalyzed reactions and their inhibition due to their unique physical and chemical properties [12-14]. Currently, three kinds of nano-materials-related approaches have been developed for enzyme activity detection: (1) The first is the use of nano-materials as enzyme carriers for loading a large amount of enzymes to enhance the detection signal [15]. Unfortunately, some of these approaches require a complex modifying process or introduce additional substrates, which make a complex detection protocol; (2) The second is the use of nano-materials as peroxidase- or oxidase-like activities catalysts to catalyze the oxidation of various substrates by enzyme-generated hydrogen peroxide (H_2O_2), including 2,2'-azino-bis(3-ethylbenzo-thiazoline-6-sulfonic acid) diammonium salt, 3,3,5,5-tetramethylbenzidine, and so on [16, 17]; (3) The third is the use of nano-materials as a direct signal source, unluckily, there are several intrinsic limitations, such as potential toxicity, intrinsic blinking and chemical instability, leading to inhibition of the activity of enzymes and environmental pollution. Therefore, it is also important to exploit excellent nano-materials for fabricating highly sensitive and selective biosensors.

A subclass of hybrid materials is metal-organic materials, which are built up by linking inorganic clusters with various organic linkers through strong bonds [18, 19].

Interaction of biomolecules with inorganic surfaces has been widely studied, as it represents a straightforward way to modify and trigger material properties for function application in various fields including sensing, nano-medicine, catalysis, therapy and many others [20-22]. Recent developments in the coordination polymers (CP) of coinage metal (such as Ag) and thiol compounds have attracted considerable attentions because of its unique physical properties and versatile applications [23, 24]. It is known that the thiol-Ag(I) CP is formed by the reaction of thiol with Ag(I), yielding polymeric one-dimensional super-molecular structure with -thiol-Ag(I)- repeated units, which is supported by thiol-Ag(I) interaction and Agrophilic Ag(I)···Ag(I) interaction [24-26]. Because of its facile preparation and interesting chain-like structure with various functional groups, thiol-Ag(I) CP shows great potential applications in bio-analysis [27, 28]. Typically, amino acids can chelate/bridge with metal atoms through their amino nitrogen and carboxylate oxygen atoms and form extended helical networks with many metal ions, while if sulfur-containing amino acids are used, thiol is mainly involved in the main coordination event [29, 30]. So far, the application of sulfur-containing amino acids-Ag(I) CP in AChE biosensing with its electro-catalytic property remains largely unexplored. Therefore, it is significant to employ sulfur-containing amino acids-Ag(I) CP-based nano-materials for the construction of electro-catalytic biosensor.

Herein, we present a simple and novel method for AChE activity and its inhibitors detection. The detection mechanism relied on three phenomena (Scheme 1): (1) So far, several studies show that the historical treatments with silver(I) complex

can act as antiseptic agents [31, 32] and a rising number of reports on newer and more efficient silver-based antimicrobial biomaterials, such as dressing, gels, films, and so on, were discovered [33-35]. These non-toxic Ag(I)-based nano-materials are very dazzling and splendid. In our study, a novel protein-mimicking *L*-Cysteine-Ag(I) hybrid nanowire (*L*-Cys-Ag(I) CP) can be prepared by a simple and green one-step non-template seed-less aqueous chemical synthetic strategy based on thiol-Ag(I) and Ag(I)···Ag(I) interaction. The prepared nanowires have abundant carboxyl (-COOH) and amine (-NH_2) groups at their surfaces, large amounts of peptide-linkages, and S-bonding silver ion inside, making them look and act like Ag-hybrid protein nanostructures. Furthermore, we further found that the protein-mimicking nanowires immobilized on graphene (GO)-modified electrode possess high electro-catalytic property to H_2O_2 reduction; (2) The reaction of acetylcholine chloride (ACh) with acetylcholinesterase (AChE) to form choline that is in turn catalytically oxidized by choline oxidase (ChOx) to produce hydrogen peroxide (H_2O_2) [36, 37]. Since the current response of as-produced H_2O_2 was proportional to the concentration of AChE, subsequently, we were able to probe AChE activity with high sensitivity and selectivity; (3) The inhibition of AChE with the aim of enhancing ACh levels is effective approach for AChE-relevant disease therapies [38-40]. Upon the inhibition of donepezil or tacrine on AChE enzyme activity, the consumption of dissolved O_2 and generation of H_2O_2 would be prevented, thus, resulting in a decrease in electrochemical signal and achieving quantitative determination of inhibitors. This work demonstrates that *L*-Cys-Ag(I) CP, a protein-mimicking nanowire, can be used

as a novel and versatile biosensing platform for the label-free and sensitive detection of H_2O_2, AChE activity and its inhibitors, which will inspire the exploration of more widespread applications of the protein-mimicking nanowire in analytical chemistry, and provide a new insight into AChE or inhibitor-relevant determination in biological environment.

2. Experimental

2.1. Reagents and Materials

Acetylcholinesterase (AChE), *L*-Cysteine (*L*-Cys), thrombin (TB), lysozyme (LZM), terminal deoxynucleotidyl transferase (TdT) and papain were obtained from Shanghai Sangon Biotechnology Co. Ltd. (Shanghai, China). H_2O_2 (30 wt%), glucose (GLC), $CaCl_2$, $AgNO_3$, acetaminophen (AP), dopamine (DA) and citric acid (CA) were purchased from Sinopharm Chemical Reagent Co. Ltd (China). Acetylcholine chloride (ACh), uric acid (UA), choline oxidase (ChOx), alkaline phosphatase (ALP) and inorganic pyrophosphatase (PPase) were obtained from the Sigma-Aldrich. Graphite powder (99.99995%, 325 mesh) was purchased from Alfa Aesar and the preparation of graphene oxide (GO) was custom-synthesized by Hummer's method [41]. All chemicals were of analytical grade without further purification. All solutions were prepared with double-distilled water (18.25 MΩ cm) from the Millipore Milli-Q system.

2.2. Apparatus

Electrochemical measurements were performed on a CHI 660E electrochemical workstation (Chenhua Instrument Company of Shanghai, China) at room temperature with a conventional three-electrode system: an Ag/AgCl electrode as the reference electrode, a platinum wire as the counter electrode and a modified glassy carbon electrode (GCE, 3 mm diameter) as the working electrode, respectively. Particle size analysis was acquired with a Malvern Zana ZS 90 Mastersizer. Fourier Transform-Infrared (FT-IR) spectra was performed on Bruker Optics Tensor 27 FT-IR Spectrometer, using KBr pellets.

2.3. Synthesis of protein-mimicking nanowire (L-Cys-Ag(I) CP)

The protein-mimicking nanowire was synthetized according to the reported procedures [26, 27]. The synthesis of *L*-Cys-Ag(I) CP was carried out in a 100 μL mixture containing freshly prepared aqueous solutions of $AgNO_3$ (1 mM, 10 μL), *L*-Cys (1 mM, 10 μL) and 80 μL double-distilled water. For full reaction of reactants, the mixture was incubated at 30 ^{o}C with gentle stirring (150 rpm) for 10 min. Afterwards, the obtained *L*-Cys-Ag(I) CP was stored at 4 °C when not in use.

2.4. Fabrication of the proposed sensor

Before modification, the GCE was polished with 1.0 and 0.3 alumina powder sequentially, and rinsed with double-distilled water, followed by sonication in ethanol and double-distilled water successively. The clean GCE was dried in a stream of

nitrogen and then was immersed into a homogeneous GO suspension (1.0 mg/mL). After that, GO was electrochemically deposited on GCE by cyclic voltammetry (CV) in an stirred GO suspension solution in the potential range of -1.5 to +0.5 V for 5 cycles at a scan rate of 10 mV/s. After dried in air, a mixture of *L*-Cys-Ag(I) CP solution (8 μL) and 0.5% nafion aqueous solution (2 μL) was coated on GO/GCE and nearly dried in a refrigerator at 4 °C. The resulting electrode (labelled for CP/GO/GCE) was stored in 0.1 M PBS (pH 7.0) at 4 °C for future use.

2.5. Sensing of H_2O_2, AChE activity and its inhibition

Sensing of H_2O_2:

Different final concentration of H_2O_2 (0, 0.2, 0.4, 0.6, 0.8, 1, 1.2, 1.4, 1.6, 2, 4, 6, 8 and 10 mM) was mixed with 0.1 M PBS (pH 7.0) and the cyclic voltammograms of the CP/GO/GCE were performed with a scan rate of 50 mV/s in the potential range from -1.2 to 0 V. To facilitate the following AChE activity analysis, a series of amperometric responses by successive addition of H_2O_2 were conducted at -0.3 V in 1 mL of stirred PBS solution.

Sensing of AChE activity and its inhibition:

Aliquots of PBS solution (0.1 M, pH 7.0, 1 mL) containing different final concentration of AChE (0, 0.001, 0.002, 0.005, 0.01, 0.02, 0.05, 0.1, 0.2, 0.3, 0.5, 0.7, 1, 1.2 U/L), ChOx (0.2 U/L), and ACh (2 mM) were equilibrated under gentle shaking at 37 °C for 30 min. Ultimately, the reaction solution was applied to further electrochemical measurements and amperometric responses recorded by using CP/GO/GCE at a working potential of -0.3 V under gentle stirring.

In the study of AChE inhibition, we initially mixed different final concentrations of inhibitors (donepezil: 0, 0.1, 0.2, 0.5, 0.8, 1, 2, 5, 8, 10, 15 nM; tacrine: 0, 0.25, 0.5, 1.25, 2, 2.5, 5, 12.5, 20, 25, 37.5, 50 nM) with AChE (0.5 U/L). The resulting solutions were incubated with a solution containing ChOx (0.2 U/L), and ACh (2 mM) under gentle shaking at 37 °C for 30 min. The following process was the same as that of AChE activity.

3. Results and discussions

3.1. Feasibility and characteristics of the assay

As a principal member of reactive oxygen species (ROS) and a byproduct of the reactions catalyzed by a large number of oxidase enzymes, hydrogen peroxide (H_2O_2) plays significant roles in pharmaceutical, biological systems, industrial, and other fields [42-44]. Therefore, efficient and dependable detection of H_2O_2 is of impressive significance and has become an important subject of current chemical research [20]. Herein, we report the preparation of a kind of protein-mimicking nanowire employing *L*-Cysteine (*L*-Cys) molecules as bridging ligand by simply mixing the precursors (*L*-Cys and Ag(I)), noted as *L*-Cys-Ag(I) CP (Scheme 1A). The present study demonstrated that the obtained *L*-Cys-Ag(I) CP could serve as an artificial peroxidase for sensitive sensing of H_2O_2, thus achieving the quantitative detection of H_2O_2. It is helpful for further development of a miniaturized and low-cost electrochemical sensing platform for H_2O_2-targeted biochemical and metabolism investigation. Now,

it is well-known that AChE can hydrolyze acetylcholine chloride (ACh) to choline, which can be oxidized to betaine with the concomitant generation of H_2O_2 in the presence of choline oxidase (ChOx) [45]. So we were able to probe AChE activity with high sensitivity and selectivity because the current response of as-produced H_2O_2 was proportional to the concentration of AChE (Scheme 1B). Upon the inhibition of inhibitor on AChE enzyme activity, the consumption of dissolved O_2 and generation of H_2O_2 would be prevented, thus, resulting in a decrease of electrochemical signal and achieving quantitative determination of inhibitors.

Herein, we have synthesized protein-mimicking nanowire for constructing electro-catalytic biosensor toward H_2O_2 and AChE assay. Scheme 1 illustrates the preparation process of *L*-Cys-Ag(I) CP and the reaction starts by mixing *L*-Cys with Ag(I), in which Ag(I) is facilitated by the thiol-Ag(I) and aurophilic Ag(I)···Ag(I) interaction. To verify this formation, characterization experiments have been employed including DLS and FT-IR spectra. DLS data revealed that the reaction of Ag(I) and *L*-Cys leads to a significant increase of the hydrodynamic radius of species in solution (Fig. 1A) and the average hydrodynamic radius of reaction products is about 451 ± 22 nm. Then, FT-IR was performed to characterize the resulting *L*-Cys and *L*-Cys-Ag(I) CP (Fig. 1B).The FT-IR spectrum of *L*-Cys displayed the presence of S-H with the weak absorption peak at 2553 cm^{-1}, but there is no peak between 2500 and 2600 cm^{-1} in FT-IR spectrum of *L*-Cys-Ag(I) CP, implying that S-H is probably displaced by S-Ag in the protein-mimicking nanowire. These results vividly proved that the protein-mimicking nanowire was synthesized successfully.

We also verified the successful modification of *L*-Cys-Ag(I) CP on GO/GCE. As illustrated in Fig. 2A, a pair of well-defined redox peaks, characteristic of a diffusion-limited redox process, was displayed. Compared with bare GCE, the cyclic voltammetry (CV) signal of $[Fe(CN)_6]^{3-/4-}$ dramatically increases with electro-deposition of GO. This may contribute to the excellent conductivity of the home-made GO, which can act as an electron conducting tunnel or electrical wire and promote the transmission of electrons between the redox probe and the underlying electrode. Moreover, the current signal sharply decreases and the reversibility becomes poorer after the modification of *L*-Cys-Ag(I) CP efficiently on the GO/GCE surface due to the inertness of amino acid (*L*-Cys) in the protein-mimicking nanowire. Electrochemical impedance spectroscopy (EIS) was employed to further monitor the modified electrodes by electron transfer resistance (R_{et}) (Fig. 2B). The bare GCE shows a small semicircle, and when GO was electrodeposited on GCE, a lower semicircle was exhibited because GO can improve the conductivity of the whole electrode surface. After *L*-Cys-Ag(I) CP was dropped onto GO/GCE, a sharp increase of R_{et} is observed owing to the non-conductive property of amino acid. These results correspond with that of aforementioned CV experiment, further indicative of the assembly of GO and *L*-Cys-Ag(I) CP on the surface of GCE.

The electro-catalytic property of *L*-Cys-Ag(I) CP plays a significant role in the proposed sensor and was monitored by CV. As depicted in Fig. 2C, two different electrolyte solutions with H_2O_2 and without H_2O_2 were prepared, there is no apparent peak current in the absence of H_2O_2, and an outstanding peak appears at -0.8 V. This

might mainly results from the *L*-Cys-Ag(I) CP toward the electro-catalytic reduction of H_2O_2. To investigate further the enhancement effect of *L*-Cys-Ag(I) CP on electro-catalytic property to H_2O_2 reduction, different modified electrodes were fabricated. As shown in Fig. 2D, the bare GCE, Ag(I)/GO/GCE and *L*-Cys/GO/GCE show no redox peaks, while a tremendous reduction peak is observed at -0.8 V for *L*-Cys-Ag(I) CP modified electrode, further proving unique electro-catalytic property of *L*-Cys-Ag(I) CP is at the root of the enhancement of the current signal.

3.2. Sensing of H_2O_2

To investigate further the unique electro-catalytic property of *L*-Cys-Ag(I) CP and the analytical performance of the proposed biosensor, CVs were performed to probe the reduction of H_2O_2 with different concentrations at CP/GO/GCE. As can be seen from Fig. 3A, the peak current of H_2O_2 reduction increases with the concentration of H_2O_2 increasing from 0 to 10 mM. There is a good linear relationship between peak current and concentration of H_2O_2 (Fig. 3B), revealing that the *L*-Cys-Ag(I) CP shows an excellent electro-catalytic property toward H_2O_2 reduction. The enhanced electro-catalytic property of CP/GO/GCE could be ascribed to the following two possible aspects: first, the protein-mimicking nanowire provides a naked electro-catalytic surface, which can act as highly active electro-catalyst; second, the fast charge transfer derived from GO with high conductivity may result in the enhancement of the electrochemical signal [46]. To test the storage stability of the

sensor, the current response to 6 mM H_2O_2 was recorded every two days. As shown in Fig. 3C, the variation of the response current at the CP/GO/GCE decreased to about 88.5% of its initial current response on the fifteenth day, indicating good stability. The specificity of the proposed sensor to H_2O_2 was also elucidated by challenging it with several substances, and the proposed sensor showed remarkably high selectivity (Fig. 3D) and good anti-interference (Fig. S1) to H_2O_2. These results indicate *L*-Cys-Ag(I) CP-based electro-catalytic biosensor is as a promising new tool for analysis of H_2O_2-related enzyme systems.

Furthermore, to convince large current density and avert the interference from other biologically active molecules, the amperometric *i-t* curve of the CP/GO/GCE with successive addition of varying concentrations of H_2O_2 in 0.1 M PBS (pH 7.0) was conducted. As shown in Fig. 4A, the protein-mimicking nanowire-derived biosensor exhibits quick response to H_2O_2 and the electrochemical signal increases with the change of H_2O_2 concentration. Moreover, as noted in Fig. 4B, there is a linear relationship over the range of 0.001 to 5 mM with a detection limit of 0.3 μM (signal-to-noise ratio of 3), which is lower than those of most of previously-reported H_2O_2 assays (Table S1). Therefore, the protein-mimicking nanowire is an ideal signal-amplifying label for H_2O_2 detection with high sensitivity. Then, the effect on some co-exciting electro-active species for the response current was evaluated at the potential of -0.3 V. As shown in Fig. 4C, a fast and obvious current response to the addition of 0.5 mM H_2O_2 was displayed, while there is no change with the discontinuous addition of uric acid (UA), dopamine (DA), citric acid (CA),

acetaminophen (AP), glucose (GLC), K^+, Ca^{2+} and Cl^- in the same case. So, these co-exciting substances have no interference in the determination of H_2O_2. Next, eight protein-mimicking nanowire-modified electrodes were investigated at 0.5 mM H_2O_2 and the negligible difference on the current-time response was displayed (Fig. 4D). To testify the feasibility of the CP/GO/GCE in practical analysis, the recovery experiment was conducted to determine the H_2O_2 content in human serum or urine, respectively. The concentration of H_2O_2 was determined using the regression equation, and the excellent recoveries results obtained for serum and urine samples are tabulated in Table S2 and Table S3. These excellent results provide a new insight into H_2O_2-relevant determination in complicated biological enzyme systems.

3.3. Probing AChE activity and its inhibitors

The function of protein-mimicking nanowire as a biosensing platform was further expanded by exploring its application in enzymatic activity analysis. In our work, the sequential chain of reactions from the ACh, AChE, ChOx, leading to detection of H_2O_2 is shown below. First, ACh is hydrolyzed by AChE, forming acetate and choline, reaction 1. Thereafter, choline can be oxidized by ChOx forming H_2O_2 and betaine aldehyde, reaction 2, which is further oxidized, forming one additional H_2O_2 and betaine, reaction 3. Finally, H_2O_2 is reduced at the protein-mimicking nanowire-based electrode, reaction 4.

$$\text{Acetylcholine(ACh)} + H_2O \rightarrow \text{Acetate} + \text{Choline} \quad (1)$$

$$\text{Choline} + O_2 \rightarrow \text{Betaine aldehyde} + H_2O_2 \quad (2)$$

$$\text{Betaine aldehyde} + O_2 + H_2O \rightarrow \text{Betaine} + H_2O \quad (3)$$

$H_2O_2+2H^++2e^-\rightarrow 2H_2O$ (4)

Following the design, the feasibility of the proposed method was investigated and the results were exhibited in Fig. S2. After the incubation of AChE with other reacting substances, the resulting reaction solution was added to the electrolyte solution for detection. In comparison with the control sample, the whole AChE-catalyzed reaction caused a significant electrochemical signal enhancement, which is about 13-fold as high as that of the control experiments. Therefore, the prepared protein-mimicking nanowire-based electro-catalytic biosensor can be explored for probing AChE activity.

To achieve the high sensitivity of the proposed AChE biosensor, we optimized the analytical parameters such as the electro-deposition cycles of GO on GCE, AChE reaction time, AChE reaction temperature, AChE reaction pH and concentration ratio of AChE/ChOx, which could affect the proposed biosensor response. The GO/GCE after electro-deposition was monitored by cyclic voltammograms with $[Fe(CN)_6]^{3-/4-}$ probe (Fig. S3), and the results indicated that the optimal electro-deposition cycle was 5 which offered high current response with the smallest anodic-to-cathodic peak separation. As shown in Fig. S4A, the relative current response enhanced with the increasing reaction time and the current response reached the maximum within 30 min. Therefore, 30 min was chosen as the optimal reaction time in this detection system. To confirm the best reaction temperature for the system, different reaction temperatures were investigated. As shown in Fig. S4B, the relative current response of the detection system changes with temperature. It was found that the current response reached the maximum when the temperature was 37 °C. Thus, 37 °C was selected as

reaction temperature in the further experiments. The relative current response of the reaction system changes under different pH conditions (Fig. S4C). When the solution pH is between 5.5 and 7.0, a small current-time response of the reaction system increase, and at pH 7.0, the current response is highest. It may be that higher pH will lead to the AChE and ChOx denatured and result in lower activity of the enzymes. It is proved that the optimum pH values for AChE was 7.0. Therefore, 0.1 M PBS (pH 7.0) was selected as the detection medium in further experiments. In order to establish a better relationship between the current responses of the reaction system, it is important to optimize the concentrations of AChE and ChOx. Fig. S4D showed the current response of the reaction system upon interaction with 2 mM ACh and different ratios of AChE/ChOx for a fixed time interval of 30 min. It can be seen that a gradual increase of the current was observed when ratios of AChE/ChOx was less than 2.5, thus later the current response showed a downward trend. Therefore, the optimal proportion of 2.5 was used in the following experiments.

Under the optimized conditions, the dynamic response range of AChE in buffer solution was recorded through electrochemical changes. As shown in Fig. 5A, a set of obvious *i-t* responses of H_2O_2 appear and the electrochemical current responses increase gradually with the increment of concentrations of AChE, implying a gradual hydrolysis reaction. Meanwhile, Fig. 5B showed a line correction between the electrochemical current and AChE concentrations, ranging from 0.001 to 1.0 U/L. According to signal-to-noise ratio of 3, the detection limit of AChE was calculated to be 0.0006 U/L, which is lower than those of most of previously-reported AChE assays

(Table 1). Thus, a novel, simple, and label-free electrochemical strategy for sensitive detection of AChE activity was developed based on unique electro-catalytic property of our proposed protein-mimicking nanowire. To evaluate the specificity of the proposed electrochemical assay toward AChE, other enzymes were investigated as control samples. None of them can produce remarkable electrochemical signal in the assay as AChE did (Fig. 5C). Moreover, the mixture anti-interference systems present good current responses (Fig. 5D). These results clearly demonstrated that this assay based on protein-mimicking nanowire could be applied for probing AChE activity with high sensitivity and selectivity.

To eliminate the interference from complex biological system, an AChE-trapping test was performed in diluted serum or urine samples spiked with different concentrations of AChE. Recovery measurement of AChE spiked in 10% serum or urine was conducted by the proposed electrochemical approach. The recoveries were in an acceptable range from 95.9 to 101.8% for serum samples (Table S4) and from 96.1 to 102.3% (Table S5) for urine samples, and the RSD was in the range from 1.9 to 4.1% for serum samples and from 2.3 to 3.8% for urine samples, indicating an acceptable accuracy.

3.4. Screening of AChE Inhibitors

Similar to the measurement of enzyme activity under normal conditions, it is possible to determine the inhibition of the enzyme, providing a facile and clear method for AChE inhibitors. Donepezil [47, 48] and tacrine [49, 50], which are widely used in

the drug of Alzheimer, were chosen as models. As exposed in Fig. 6A and Fig. 6C, the electrochemical signal of the system decreased gradually with the increment of the concentration of donepezil or tacrine, but a strong electrochemical reduction response was observed without donepezil or tacrine. On the basis of the plot of electrochemical signal *versus* the concentration of donepezil (Fig. 6B) and tacrine (Fig. 6D), the corresponding IC_{50} (the inhibitor concentration required for 50% inhibition of the enzyme activity) is determined to be about 1.4 nM and 3.5 nM, respectively, which is similar to those obtained by other AChE assays [47-50]. Thus, these results clearly suggest that the proposed assay has a considerable potential to qualitatively screen AChE inhibitors and provides a broad prospect for AChE-based drug discovery.

4. Conclusion

In conclusion, the present study developed a simple and sensitive method for sensing of H_2O_2, AChE and its inhibitors based on *L*-Cys-Ag(I) CP. *L*-Cys-Ag(I) CP is *in-situ* synthetized via thiol-Ag(I) and Ag(I)···Ag(I) interaction, and looks and acts like protein-mimicking nanowire due to massive *L*-Cysteines. Moreover, the nanowire possesses unique electro-catalytic property to H_2O_2 reduction. The H_2O_2 detection platform was then implemented to detect AChE activity and its inhibitors based on the production of H_2O_2 of AChE-catalyzed hydrolysis. The resulting electro-catalytic biosensor showed high sensitivity and selectivity for H_2O_2 or AChE and its inhibitors detection. The proposed electro-catalytic platform displays a new function of protein-mimicking nanowire and provides a versatile direction for the label-free detection of H_2O_2 and enzyme activity.

Acknowledgements

Financial support from the National Natural Science Foundation of China (21605089, 41576098 and 81773483), the Ningbo Municipal Natural Science Foundation (2017A610228, 2016A610052 and 2016A610205), the Open Subject of State Key Laboratory of Chemo/Biosensing and Chemometrics (2016001) and Project of Academic Research Foundation of Ningbo University (XYL17002) are gratefully acknowledged. This work was also sponsored by K.C. Wong Magna Fund in Ningbo University.

References

[1] D. M. Quinn, Chem. Rev. 87 (1987) 955-979.

[2] M. Schumacher, S. Camp, Y. Maulet, M. Newton, K. Macphee-Quigley, S. S. Taylor, T. Friedmann, P. Taylor, Nature 319 (1986) 407-409.

[3] P. Taylor, Z. Radić, Annu. Rev. Pharmacol. Toxicol. 34 (1994) 281-320.

[4] J. L. Sussman, M. Harel, F. Frolow, C. Oefner, A. Goldman, L. Toker, I. Silman, Science 253 (1991) 872-879.

[5] K. I. Hawkins, C. E. Knittle, Anal. Chem. 44 (1972) 416-417.

[6] L. Saa, R. Grinyte, A. Sánchez-Iglesias, L. M. Liz-Marzán, V. Pavlov, ACS Appl. Mater. Interfaces 8 (2016) 11139-11146.

[7] R. Zhang, N. Li, J.Y. Sun, F. Gao, J. Agric. Food Chem. 63 (2015) 8947-8954.

[8] C. Y. Lei, Z. Wang, Z. Nie, H. H. Deng, H. P. Hu, Y. Huang, S. Z. Yao, Anal.

Chem. 87 (2015) 1974-1980.

[9] T. W. Kang, S. J. Jeon, H. I. Kim, J. H. Park, D. B. Yim, H. R. Lee, J. M. Ju, M. J. Kim, J. H. Kim, ACS Nano 10 (2016) 5346-5353.

[10] X. Y. Ouyang, P. E. G. Leonards, Z. Tousova, J. Slobodnik, J. Boer, M. H. Lamoree, Anal. Chem. 88 (2016) 2353-2360.

[11] H. M. Chen, H. Zhang, R. Yuan, S. H. Chen, Anal. Chem. 89 (2017) 2823-2829.

[12] E. Hutter, D. Maysinger, Trends Pharmacol. Sci. 34 (2013) 497-507.

[13] A. L. Hu, H. H. Deng, X. Q. Zheng, Y. Y. Wu, X. L. Lin, A. L. Liu, X. H. Xia, H. P. Peng, W. Chen, G. L. Hong, Biosens. Bioelectron. 97 (2017) 21-25.

[14] Y. P. Jiang, W. H. Luo, X. P. Wang, Y. H. Lin, X. Y. Liu, RSC Adv. 6 (2016) 33132-33137.

[15] W. Jiang, X. H. Wang, J. W. Chen, Y. Liu, H. B. Han, Y. Ding, Q. S. Li, J. Tang, ACS Appl. Mater. Interfaces 9 (2017) 26948-26957.

[16] D. Huber, G. Tegl, A. Mensah, B. Beer, M. Baumann, N. Borth, C. Sygmund, R. Ludwig, G. M. Guebitz, ACS Appl. Mater. Interfaces 9 (2017) 15307-15316.

[17] K. Chang, Z. H. Liu, X. F. Fang, H. B. Chen, X. J. Men, Y. Yuan, K. Sun, X. J. Zhang, Z. Yuan, C. F. Wu, Nano Lett. 17 (2017) 4323-4329.

[18] X. Kuang, Y. Ma, H. Su, J. Zhang, Y. B. Dong, B. Tang, Anal. Chem. 86 (2014) 1277-1281.

[19] H. T. Li, F. Guo, M. Kou, A. Famulari, Q. Fu, J. Marti-Rujas, Inorg. Chem. 56 (2017) 6584-6590.

[20] C. Sanchez, K. J. Shea, S. Kitagawa, Chem. Soc. Rev. 40 (2011) 471-472.

[21] Y. Razvag, V. Gutkin, M. Reches, Langmuir 29 (2013) 10102-10109.

[22] J. P. Palafox-Hernandez, Z. H. Tang, Z. E. Hughes, Y. Li, M. T. Swihart, P. N. Prasad, T. R. Walsh, M. R. Knecht, Chem. Mater. 26 (2014) 4960-4969.

[23] X. Yuan, Y. Q. Tay, X. Y. Dou, Z. T. Luo, D. T. Leong, J. P. Xie, Anal. Chem. 85 (2013) 1913-1919.

[24] B. Bellina, I. Compagnon, F. Bertorelle, M. Broyer, R. Antoine, P. Dugourd, J. Phys. Chem. C 115 (2011) 24549-24554.

[25] I. G. Dance, L. J. Fitzpatrick, A. D. Rae, M. L. Scudder, Inorg. Chem. 22 (1983) 3785-3788.

[26] J. S. Shen, D. H. Li, M. B. Zhang, J. Zhou, H. Zhang, Y. B. Jiang, Langmuir 27 (2011) 481-486.

[27] W. J. Chen, L. Y. Zheng, M. L. Wang, Y. W. Chi, G. N. Chen, Anal. Chem. 85 (2013) 9655-9663.

[28] F. F. Cao, E. G. Ju, C. Q. Liu, F. Pu, J. S. Ren, X. G. Qu, Chem. Commun. 52 (2016) 5167-5170.

[29] K. Katagiri, T. Sakai, M. Hishikawa, H. Masu, M. Tominaga, K. Yamaguchi, I. Azumaya, Cryst. Growth Des. 14 (2014) 199-206.

[30] L.Y. Du, W. J. Shi, L. Hou, Y. Y. Wang, Q. Z. Shi, Z. Zhu, Inorg. Chem. 52 (2013) 14018-14027.

[31] H. J. Klasen, Burns 26 (2000) 117-130.

[32] H. J. Klasen, Burns 26 (2000) 131-138.

[33] J. Gu, Y. J. Su, P. Liu, P. Li, P. Yang, ACS Appl. Mater. Interfaces 9 (2017)

198-210.

[34] H. L. Cao, Y. Q. Qiao, F. H. Meng, X. Y. Liu, J. Phys. Chem. Lett. 5 (2014) 743-748.

[35] J. López-Esparza, L. F. Espinosa-Cristóbal, A. Donohue-Cornejo, S. Y. Reyes-López, Ind. Eng. Chem. Res. 55 (2016) 12532-12538.

[36] J. D. Keighron, S. Åkesson, A. S. Cans, Langmuir 30 (2014) 11348-11355.

[37] Y. Xu, T. Yu, X. Q. Wu, J. S. Shen, H. W. Zhang, RSC Adv. 5 (2015) 101879-101886.

[38] F. Feng, Y. Tang, S. Wang, Y. Li, D. Zhu, Angew. Chem. Int. Ed. 46 (2007) 7882-7886.

[39] T. Tian, X. S. Li, J. C. Cui, J. Li, Y. Lan, C. Wang, M. Zhang, H. Wang, G. T. Li, ACS Appl. Mater. Interfaces 6 (2014) 15456-15465.

[40] M. Cuartero, M. S. García, F. García-Cánovas, J. Á. Ortuño, Talanta 110 (2013) 8-14.

[41] W. S. William, J. R. Hummers, E. O. Richard, J. Am. Chem. Soc. 80 (1958) 1339.

[42] J. K. Edwards, S. J. Freakley, A. F. Carley, C. J. Kiely, G. J. Hutchings, Acc. Chem. Res. 7 (2014) 845-854.

[43] R. Q. He, H. F. Tang, D. C. Jiang, H. Y. Chen, Anal. Chem. 88 (2016) 2006-2009.

[44] H. H. Zeng, W. B. Qiu, L. Zhang, R. P. Liang, J. D. Qiu, Anal. Chem. 88 (2016) 6342-6348.

[45] F. Wang, X. Liu, C. H. Lu, I. Willner, ACS Nano 7 (2013) 7278-7286.

[46] V. Georgakilas, J. N. Tiwari, K. C. Kemp, J. A. Perman, A. B. Bourlinos, K. S. Kim, R. Zboril, Chem. Rev. 116 (2016) 5464-5519.

[47] E. A. Van der Zee, B. Platt, G. Riedel, Behav. Brain Res. 221 (2011) 583-586.

[48] F. Ibrahim, Y. C. Guillaume, M. Thomassin, C. André, Talanta 79 (2009) 804-809.

[49] M. Wang, X. G. Gu, G. X. Zhang, D. Q. Zhang, D. B. Zhu, Langmuir 25 (2009) 2504-2507.

[50] Y. D. Zhang, Y. N. Cai, Z. L. Qi, L. Lu, Y. X. Qian, Anal. Chem. 85 (2013) 8455-8461.

Scheme 1 Schematic diagrams of (A) the synthesis of protein-mimicking nanowire (*L*-Cys-Ag(I) coordination polymer) and (B) the electro-catalytic biosensor for probing AChE activity.

Fig. 1 (A) Size distributions of *L*-Cys and *L*-Cys-Ag(I) CP determined by dynamic light scattering (DLS); (B) FT-IR spectrums of *L*-Cys and *L*-Cys-Ag(I) CP.

Fig. 2 (A) Cyclic voltammogram and (B) electrochemical impedance spectroscopy (EIS) of the bare GCE, GO/GCE and CP/GO/GCE in 5 mM $[Fe(CN)_6]^{3-/4-}$ containing 0.1 M KCl; (C) Cyclic voltammograms of CP/GO/GCE in the presence or absence of 6 mM H_2O_2; (D) Cyclic voltammograms of GCE, Ag(I)/GO/GCE, *L*-Cys/GO/GCE and CP/GO/GCE in 0.1 M PBS (pH 7.0) containing 6 mM H_2O_2.

Fig. 3 (A) Cyclic voltammograms of the CP/GO/GCE in 0.1 M PBS (pH 7.0) with increasing H_2O_2 concentration; (B) The relationship between the current response and

the concentration of H_2O_2; (C) Stability of the proposed electrochemical sensors within two weeks; (D) Selectivity of the electrochemical H_2O_2 sensor based on *L*-Cys-Ag(I) CP, the concentration of all analysts is 6 mM.

Fig. 4 (A) Current-time response obtained in 0.1 M PBS (pH 7.0) by increasing different concentrations of H_2O_2 on the CP/GO/GCE at -0.3 V; (B) The plot of response current *vs.* the concentration of H_2O_2; (C) Current-time at CP/GO/GCE for the successive addition of 0.5 mM H_2O_2, but alternation of 1 mM UA, DA, CA, AP, GLC, Ca^{2+}, K^+ or Cl^-; (D) The repeatability of the proposed electrochemical AChE sensors.

Fig. 5 (A) Current-time in response to different final concentrations of AChE (from 0 to 1.2 U/L); (B) Calibration curve of the proposed AChE sensor; (C) Selectivity and (D) Interference of the prepared AChE sensor, the concentration of all analysts is 0.5 U/L.

Fig. 6 (A) Various final concentrations of donepezil were used for investigation of AChE inhibition; (B) Electrochemical signal as a function of the concentration of donepezil; (C) Various final concentrations of tacrine were used for investigation of AChE inhibition; (D) Electrochemical signal as a function of the concentration of tacrine.

Table 1 The comparison of our electrochemical method with other methods on AChE activity detection.

Sensors	Detection limit (U/L)	Linear range (U/L)	Reference
$H_{39}GFP/Cu^{2+}$	0.015	0.025 ~ 2	Anal. Chem. 87 (2015) 1974-1980
Functional monomer	5	10 ~ 10000	ACS Appl. Mater. Interfaces 6 (2014) 15456-15465

Carbon dots	1	1 ~ 80	Colloid. Surface. B 125 (2015) 90-95
Ag(I) ions-TMB	0.0043	0 ~ 0.03	Sensor. Actuat. B Chem. 226 (2016) 104-109
Perylene probe	0.04	0 ~ 40	Anal. Chem. 85 (2013) 2667-2672
Fe_3O_4/AuNPs	0.02	0.05 ~ 5.0	Biosens. Bioelectron. 26 (2011) 4231-4235
DNA-Cu/AgNCs	0.05	0.05 ~ 2.0	Biosens. Bioelectron. 47 (2013) 345-349
Ag@SiO_2NPs-HPTS	0.05	0 ~ 5.0	Biosens. Bioelectron. 68 (2015) 648-653
$PTCOO^-$	200	200 ~ 1500	ACS Appl. Mater. Interfaces 3 (2011) 1306-1310
AuNPs	0.6	0.6 ~ 2.0	Langmuir 25 (2009) 2504-2507
dC_{12}-AgNCs	0.05	0.1 ~ 1.25	Anal. Chem. 85 (2013) 8455-8461
L-Cys-Ag(I) CP/GO/GCE	0.0006	0.001 ~ 1	This work

Highlights

- The synthetized *L*-Cys-Ag(I) CP looks like Ag-hybrid protein nanostructures.
- The protein-mimicking nanowire exhibits excellent electro-catalytic property.
- The biosensor was applied for AChE activity detection and inhibitors screening.
- The platform displays great potential applications in biologic environments.

Scheme 1

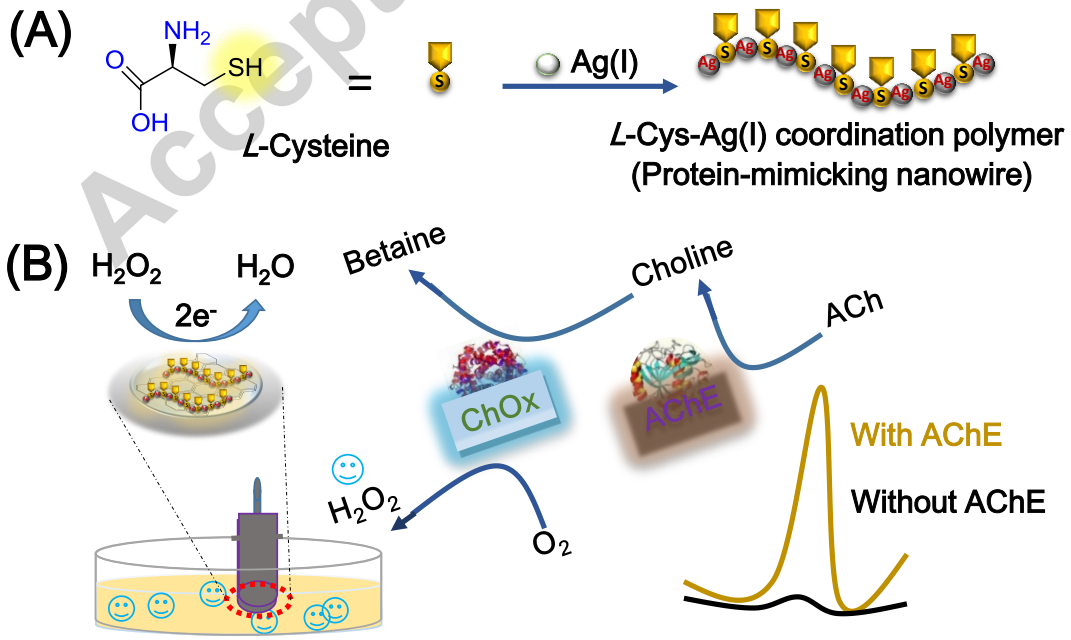

Fig. 1

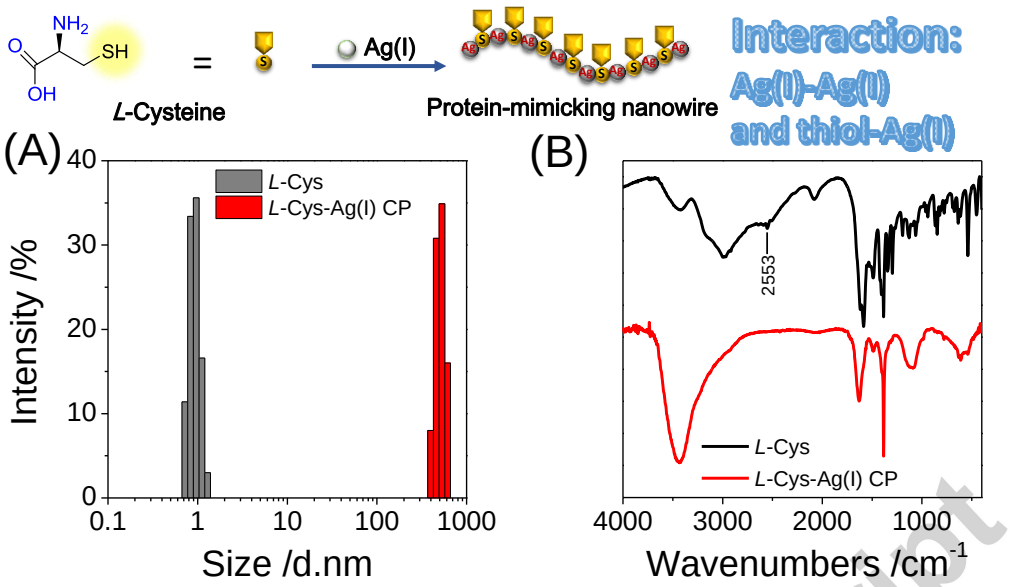

Fig. 2

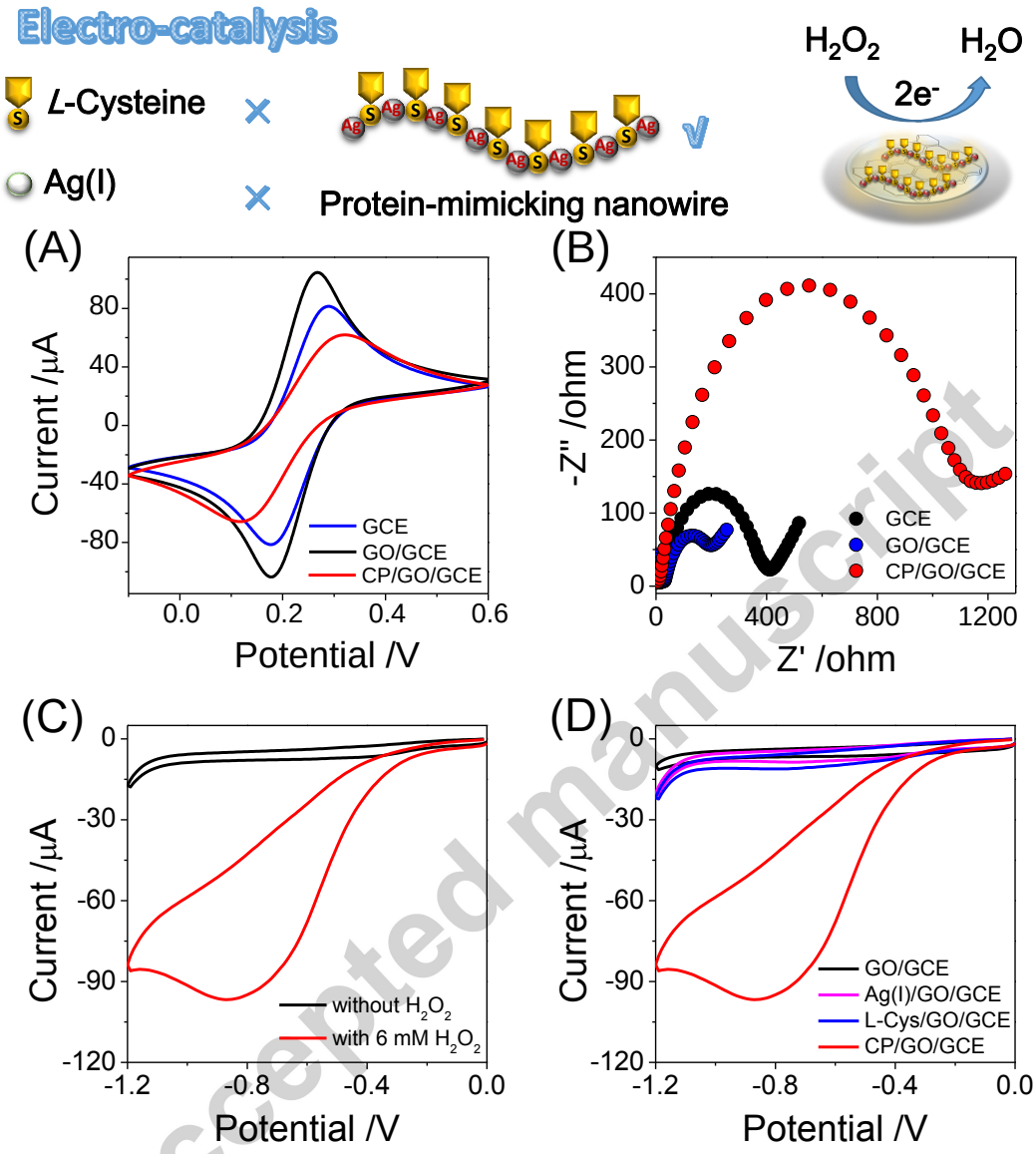

Fig. 3

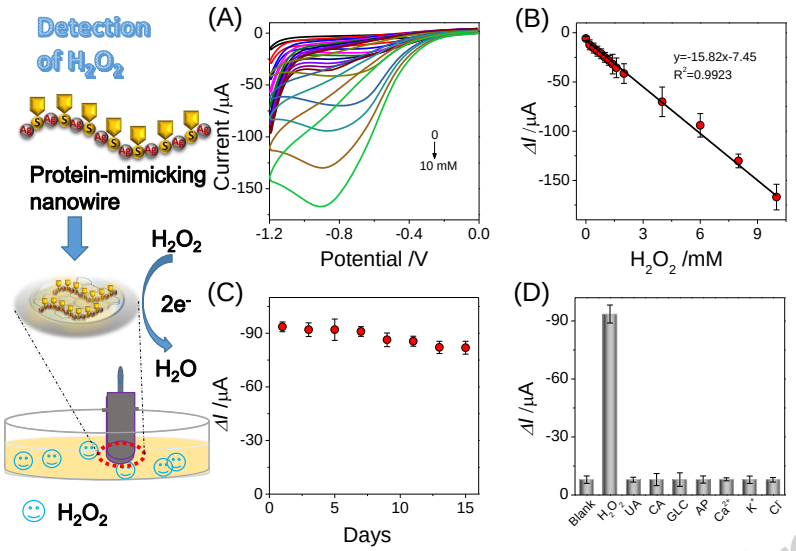

Fig. 4

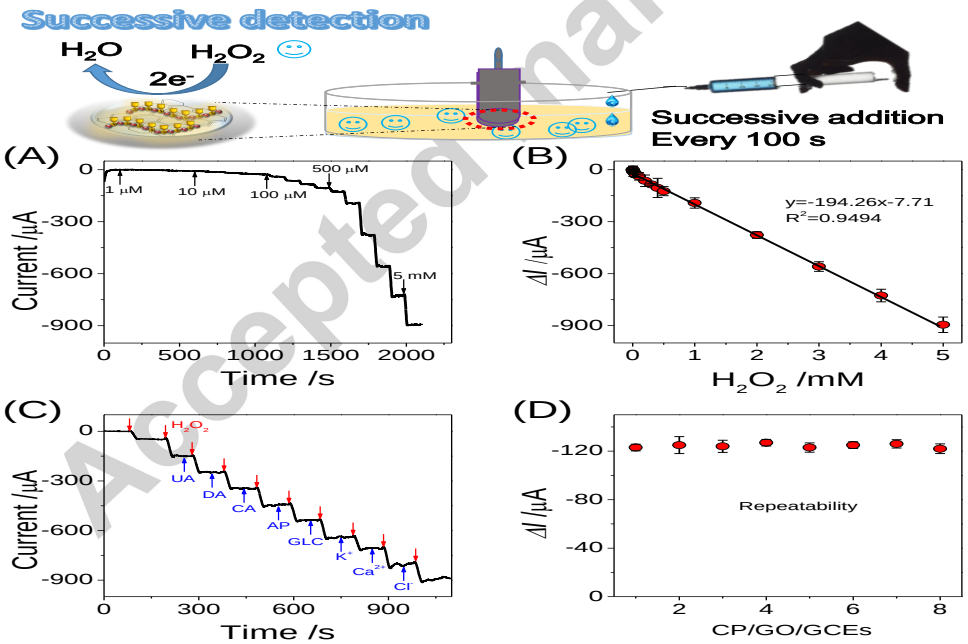

Fig. 5

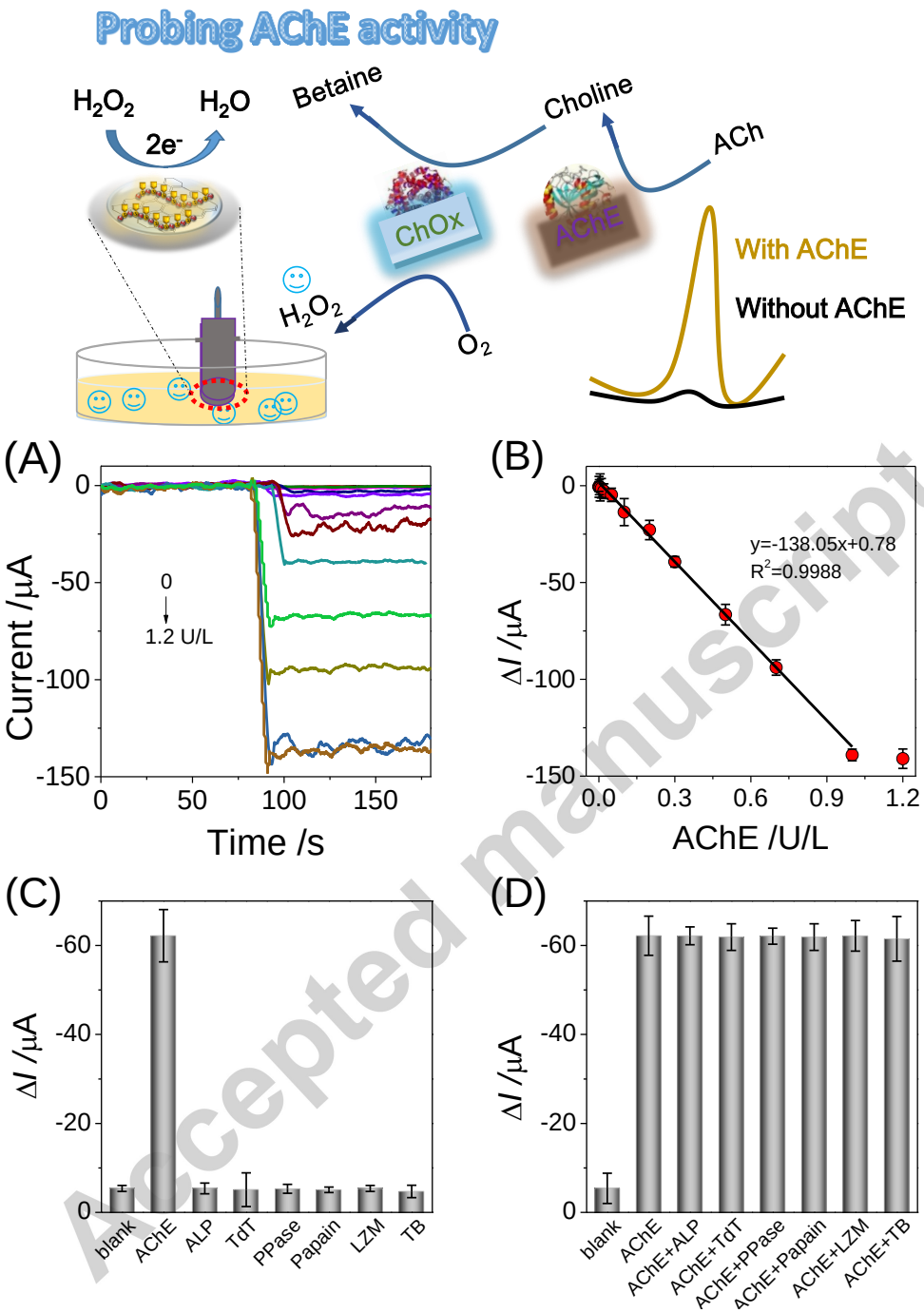

Fig. 6